Surface Characterization of Poly 2-Vinylpyridine - A Polymer for Area Selective Deposition Techniques

M. Snelgrove[2], C. Zehe[2], R. Lundy[3], P. Yadav [3], J.-P. Rueff[4,5], R. O'Connor[2], J. Bogan[2], G. Hughes[2,6], E. McGlynn[2,6], M. Morris[3], P.G. Mani-Gonzalez[1]

[1]*Instituto de Ingeniería y Tecnología, Departamento de Física y Matemáticas, Universidad Autónoma de Ciudad Juárez, Ave. Del Charro 450, Cd. Juárez C.P. 32310, Chihuahua. México.*
[2]*School of Physical Sciences, Dublin City University, Glasnevin, Dublin 9, Ireland*
[3]*AMBER, Trinity College Dublin, College Green, Dublin 2, Ireland*
[4]*Synchrotron SOLEIL L'Orme des Merisiers, BP 48 Saint-Aubin, 91192 Gif-sur-Yvette, France*
[5]*Sorbonne Université, CNRS, Laboratoire de Chimie Physique - Matiére et Rayonnement, LCPMR, F-75005 Paris, France*
[6]*National Centre for Plasma Science and Technology, Dublin City University, Glasnevin, Dublin 9, Ireland*

I. Abstract

Thin films of OH terminated poly-2-vinylpyridine (P2VP-OH), a polymer with potential for infiltration mediated thin film deposition, area selective deposition (ASD) and small feature size development via block copolymer (BCP) self-assembly, has been studied with hard X-Ray photoelectron spectroscopy (HAXPES). From the N 1*s* and C 1*s* core level spectra, accurate values for the binding energy positions of the species present in the films were obtained, providing clear evidence for signals associated to pyridine bonds. The aromatic ring on the P2VP side chain is clearly identified in the studied core levels. These observations allow for a complete understanding of the chemical environment of the polymer and provide evidence of the potential reactions that can occur with metal diffusion into P2VP. Transmission Electron Microscopy (TEM), Attenuated Total Reflection Infrared Spectroscopy (ATR IR) and Atomic Force Microscopy (AFM) measurements reveal high quality films and this work provides a reference base for this functional material in terms of its utility for ASD, BCP and subsequent atomic layer deposition (ALD) based polymer infiltration processes.

II. Introduction

The limitations of traditional optical lithographic patterning is a well documented concern in the semiconductor industry[1]. The study of polymers as potential materials for use in ASD has become a major field of research for developing alternative methods of nanoelectronic fabrication via the

acceptance and blocking of infiltrating metals in a variety of different polymer types[2,3]. This range includes polymers such as polystyrene (PS), poly(methyl methacrylate) (PMMA), poly(ethyleneoxide) (PEO) and poly(vinylpyridine) (PVP) [4–8].

P2VP is a leading material in ASD and BCP research, being a pH-responsive component[9,10], while also demonstrating effective segregation when used in a block co-polymer architecture with materials such as PS and polyisoprene[11], a crucial aspect of BCP morphology[12]. P2VP has had promising experimental results, being reported to facilitate the fabrication of small and uniform features such as gold nanoparticles[13]. PS-b-P2VP has been used to create small device-like structures as reported by Morris and others[14,15]. The presence of an unshared electron pair on the nitrogen atom of the pyridine ring can facilitate coordination bonding with various species such as metal-ligand complexes[16–18]. These factors make P2VP an ideal starting material for infiltration processes, such as ALD, that yield key device elements such as metallic contacts and high-k dielectrics.

Although reported in ASD studies, in-depth photoemission analysis of P2VP films and other common BCP-relevant polymers is limited. The use of polymers for the fabrication of thin films highlights the need for more intricate studies of their surface properties to allow for a better understanding of the material chemistry of complex, chemistry rich, processes, such as ALD[19]. Sequential infiltration synthesis (SIS) ALD has been reported in the literature as a particularly successful method of infiltration for a range of polymers[20–22].

The present work focuses on a hard energy X-ray photoelectron spectroscopy (HAXPES) and subsequent angle resolved HAXPES (ARHAXPES) study of the polymer P2VP. The synchrotron radiation provides high resolution photoemission spectra, allowing for accurate determination of the chemistry of the polymer, while the ARHAXPES method characterizes the thickness and depth-resolved composition of the polymer[23,24].

The nitrogen atom in the pyridine ring of P2VP (see schematic in figure 1) has a localized lone pair of electrons that can interact with other atoms via sigma and pi-pi* interactions[25]. In the case of N pyridine-metal complexes, the electron lone pair on the nitrogen is involved in the bonding interaction. Our previous work presented evidence for Cu metal ion infiltration and coordination with pyridine via liquid phase salt solution processing[26]. The role of the electron lone pair is of critical importance in facilitating the coordination bond formation with the infiltrating metal and

this is not thoroughly explored in photoemission reports to date[27]. In this letter, we report HAXPES measurements including the ARHAXPES dependence of the C 1*s* and N 1*s* signals originating from the P2VP film.

III. Experimental

P2VP films of 0.2 wt% were prepared by dissolving P2VP-OH polymer in tetrahydrofuran (THF) and subsequently spin coating at 3000 rpm for 30 seconds onto Si substrates following the process used in ref [28]. P2VP-OH is a hydroxyl chain terminated polymer brush-like system which can be coordinated to a silicon oxide surface through a condensation process[29,30].

HAXPES measurements were undertaken at SOLEIL Synchrotron at the GALAXIES beamline. Spectra were acquired at pressures of 1×10^{-9} mbar with photon beam energies of 3 keV. A Si(111) monochromator was used for the 3 keV beam. The angles chosen for ARHAXPES was in the range of 85 – 25 degrees, in intervals of 10 (with normal emission being 90 degrees). The sample position at every angle was calibrated to ensure that the photoelectron counts were at their maximum value. The fitting of the photoemission data was performed by AAnalyzer®, a program that allows for the simultaneous peak fitting of data acquired at all take-off angles[31]. For all of our studies, the use of simultaneous methods is of high importance[32]. Calculations of the thickness and chemical composition of each layer were obtained using the MLM (Multi Layer Method)[33–35].

High resolution TEM experiments to obtain the thickness of the P2VP-OH layer were performed on a FEI OSIRIS TEM, with sample preparation performed in a FEI Helios Nanolab 450 S. The sample was capped with Pt via a gas injection system.

Grazing-angle ATR IR spectroscopy was performed using a Harrick VariGATR accessory on a Nicolet iS50 spectrometer (unpolarised, angle of incidence is 65°, 32 scans, resolution 8 cm^{-1}). AFM was used to analyze the P2VP-OH surface roughness on a Bruker Dimension 3100 AFM.

IV. Results

The measured ARHAXPES spectra of the P2VP-OH film are shown in figure 1, with all spectra being shifted so that the Si^0 peak on the Si 2*p* signal (figure 1a)) occurs at 99.4 eV binding energy[35]. Si^{4+} was observed at 103.4 eV. Figure 1b) shows the N 1*s* fit, where C-N=C bonds (N-Pyridine) are the main component of the peak, occurring at 399.8 eV, while N-C at 400.9 eV was also

included in the fit[36,37]. Another signal at 399.2 eV was associated with pyridine – hydrogen interaction ($C=NH^+$-C bonds). Similar binding energy components in the N 1*s* signal have been reported in literature but have so far remained uncategorized[38,39].

The O 1*s* signal was fitted with four signals (figure 1 c)). The most prominent signal at 532.8 eV is associated to silicon oxide, which is located at the interface between P2VP-OH and the silicon wafer. The other three signals were associated with oxygen in polymer chain bonds, residual oxygen, and adsorbed surface oxygen at 530.6 eV, 532 eV and 533.3 eV respectively.

The C 1*s* signal in figure 1 d) was fitted with five signals, one of them at 285 eV being associated to C-C bonds within the polymer chain as reported by Briggs et al[40]. The signal with the highest intensity, observed at 285.7 eV is characteristic of pyridinic carbon[41,42]. The C-O signal at 286.5 eV was associated to oxygen bonding to the polymer chain and sub oxides at the interfaces. The signals for C=O and O-C=O at 287.6 eV and 288.7 eV were attributed to surface and residual oxygen[43,44]. The peak fitting parameters for the signals associated with P2VP-OH are displayed in table 1.

Core Level Peak	***hv (ev)***	**Gaussian (eV)**	**Lorentzian (eV)**	**Chemical Environment**	**Binding Energy (eV)**
C *1s*	3000	1.11	0.27	C-C	285.0
				C-Pyridine	285.7
N *1s*	3000	1.13	0.51	$C=NH^+$-C	399.2
				N-Pyridine	399.8

Table 1. Binding energy and peak fit parameters for the P2VP film.

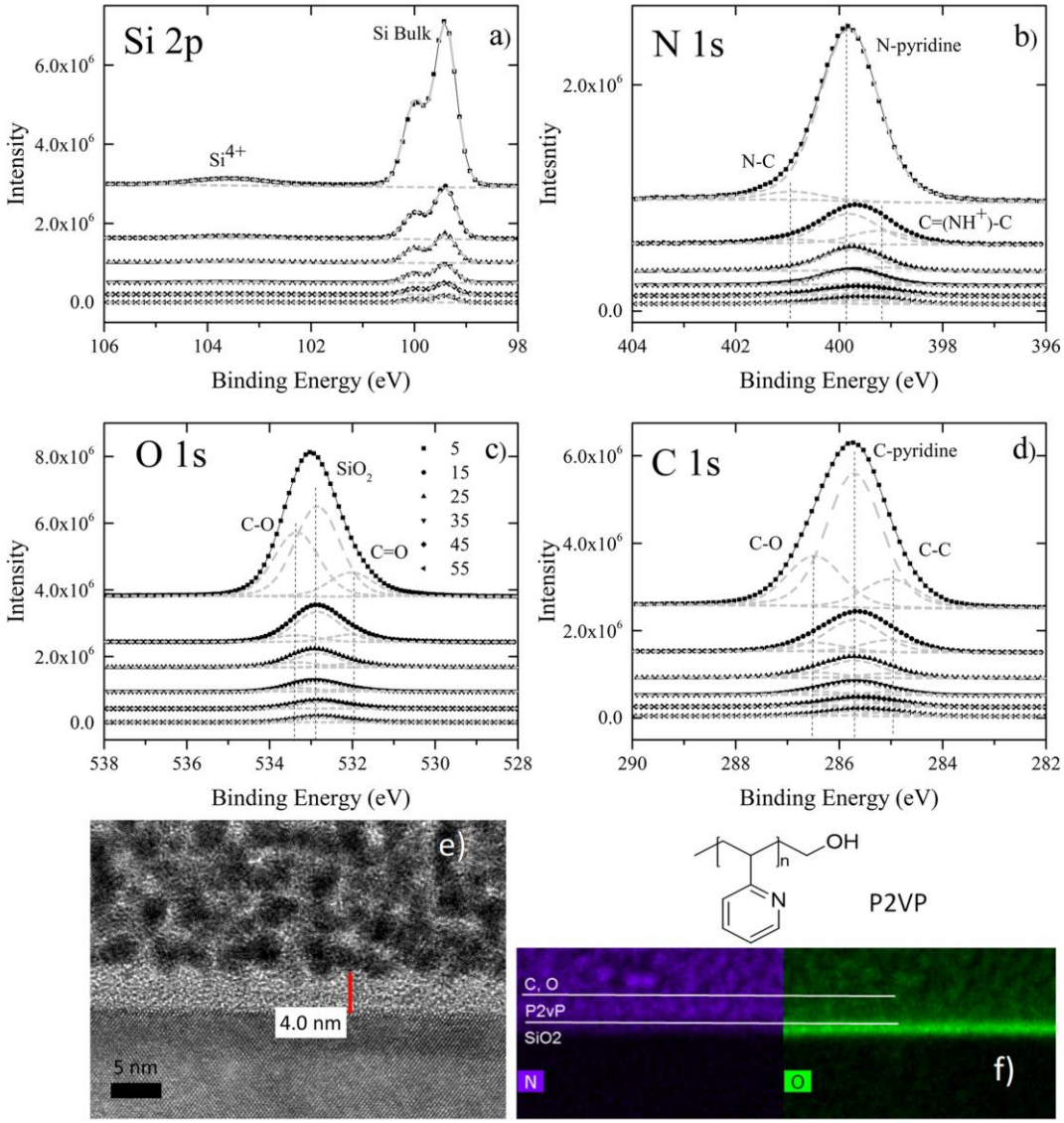

Figure 1. a) Si 2*p*, b) N 1*s*, c) O 1*s* and d) C 1*s* core level AR HAXPES of C/P2VP/SiO_2/Si scenario. e) TEM cross-sectional image of P2VP film. f) EDX mapping by TEM of P2VP film for N and O signals.

By using AR HAXPES, the thickness of the different layers present in the sample were obtained. For each core level signal (N 1*s*, Si 2*p*, C 1*s*, O 1*s*) the attenuation length of electrons, cross section, areal density, and lattice constant were considered. The assumed composition of the material for theoretical modeling was a layered C/P2VP/SiO_2/Si structure. The thickness calculations were performed using the MLM with the XPS intensity of each species that depends on the take-off

angle[45]. The band gap and density of P2VP-OH used for the calculations was 2.25 eV and 1.257 g/cm^3 respectively in accordance with literature[46,47].

The ARHAXPES results are shown in Figure 2. The P2VP and SiO_2 dependences were obtained with the C-Pyridine and Si^{4+} signals respectively. The uncertainty of the experimental data represents the variation in signal intensity across individual scans. The proposed structure of the analyzed material is presented in the inset of figure 2 a), featuring a C layer above the P2VP-OH film, which itself is above a SiO_2 layer on top of the Si bulk. The intensity of the signals associated with the films were divided by the silicon bulk intensity. This was then plotted against take off angle. Comparing the raw data with the theoretical model (MLM), stoichiometry and thickness of the thin layers were obtained.

The thicknesses determined were 1.00 ± 0.03, 3.54 ± 0.06 and 0.92 ± 0.01 nm for silicon oxide, P2VP and adventitious carbon layers respectively. The error was determined by considering two scenarios; when the intensity ratio of the films over the bulk was at maximum, and when it was at minimum. TEM images were correlated to photoemission results as shown in Figure 1 e), showing a thin film of around 4 nm on top of a silicon dioxide layer. Energy-dispersive X-ray spectroscopy (EDX) mapping by TEM provides evidence that nitrogen is present in this P2VP region (see Figure 1f)). The stoichiometry of the layers was consistent for each layer according to the chemical composition.

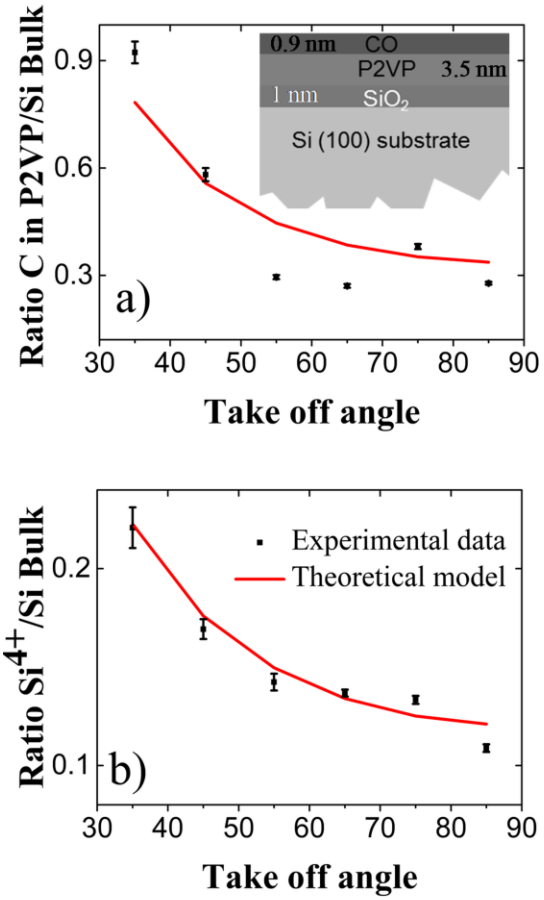

Figure 2. Angle Resolved HAXPES dependence a) Carbon in P2VP layer, and b) Si^{4+} in silicon oxide layers. The thickness and chemical composition calculation of each chemical species was considered in the sample.

Grazing-angle ATR IR spectroscopy allowed the acquisition of IR spectra even from the ultrathin P2VP-OH film used in this work, after subtracting the silicon background signal. The resulting spectrum is shown in Figure 3 a). The bands at 2927 cm^{-1} and 2854 cm^{-1} correspond to the vibrational mode of the aliphatic polymer backbone. Deformations in the free backbone lead to the signals at 1473 cm^{-1} and 1436 cm^{-1}. The stretching modes of the pyridine ring are located at 1592 cm^{-1} and 1570 cm^{-1} with an additional ring deformation band at 987 cm^{-1}[148]. The feature at 787 cm^{-1} corresponds to out-of-plane deformations of the hydrogen atoms of the pyridine ring. It is shifted to slightly higher frequencies compared to 1,2-substituted aromatic rings due to the higher electronegativity of the nitrogen atom. The signals at 1233 cm^{-1} and 1153 cm^{-1} correspond to C-O-C and C-OH vibrations respectively, resulting from the terminating hydroxy groups of the

polymer. These data indicate that partial condensation of the hydroxy group with the hydroxy functionalized silicon substrate may occur during film deposition. This hypothesis agrees with the observation of a visible band at 891 cm^{-1} corresponding to a Si-C bond vibration[49].

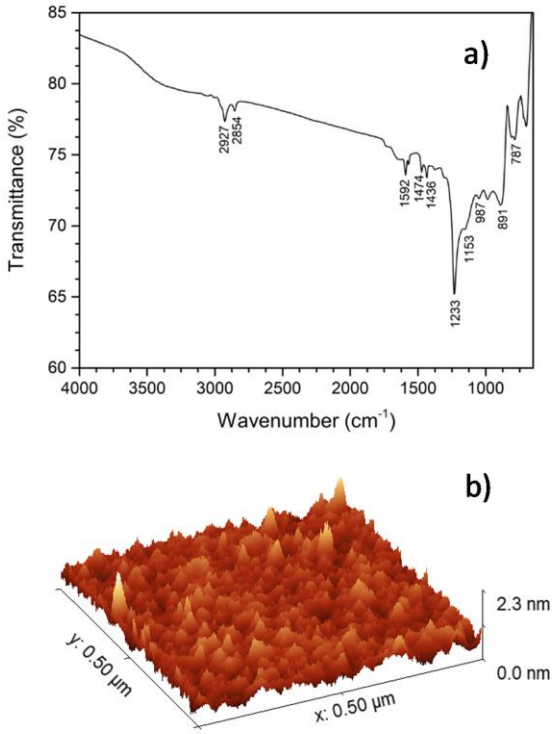

Figure 3. a) Grazing-angle ATR IR spectrum of a thin P2VP film. b) AFM 3D height image of P2VP surface.

AFM measurements were also performed on the analyzed P2VP-OH samples to assess the physical surface profile of the spun-on polymer film (figure 3 b)). The average root-mean-square (RMS) surface roughness of the P2VP-OH according to AFM analysis was approximately 0.21 nm, which indicates the presence a very smooth film and similar to values obtained for the Si substrate.

V. Conclusion

In summary, we have investigated P2VP-OH with a 3 keV HAXPES photon beam, resulting in a non-destructive and high resolution chemical analysis of the film. The P2VP-OH signals were deconvoluted in a robust and highly detailed process. The ARHAXPES analysis of the polymer indicates that the pyridine N will facilitate metal incorporation into the film, with the N 1*s* showing

a signal corresponding to H reaction with the N-pyridine lone pair, which has not yet been reported to our knowledge. Our results suggest a change in binding energy corresponds with the lone pair interactions. ARHAXPES and TEM confirm the presence of a uniform thin film of the polymer. The IR spectroscopy indicates the condensation incorporation of the P2VP-OH into the substrate. The work in this letter should act as a reference for future work on this polymer in ASD and BCP infiltration studies.

VI. Acknowledgments

This work was supported by CONACyT fund 2018-000007-01EXTV-00235. The synchrotron measurements were performed at the GALAXIES beamline with approval from SOLEIL (proposal number 20180106). We also appreciate the technical support from Matt Shaw, Jennifer Mckenna Alan Bell, Christopher O'Neill and David Bird at Intel Ireland, Leixlip. Helpful advice and GA-ATR IR measurements by Mark Croke and David James from Thermo Fisher Scientific are gratefully acknowledged. This publication has emanated from research conducted with the financial support of Science Foundation Ireland (SFI) under grant number 12/RC/2278 and 16/SP/3809.

VII. References

1. R. A. Segalman, Mat. Sci. Eng. R. **48**, 191 (2005).

2. X. Jiang, and S. F. Bent, J. Electrochem. SOC. **154**, D648 (2007).

3. R. Chen, H. Kim, P. C. McIntyre, and S. F. Bent, Appl. Phys. Lett. **84**, 4017 (2004).

4. R. Lundy, S. P. Flynn, C. Cummins, S. M. Kelleher, M. N. Collins, E. Dalton, S. Daniels, M. A. Morris, and R. Enright, Phys. Chem. Chem. Phys. **19**, 2805 (2017).

5. Q. Peng, Y.-C. Tseng, S. B. Darling, and J. W. Elam, Adv. Mater. **22**, 5129 (2010).

6. D. Borah, M. T. Shaw, S. Rasappa, R. A. Farrell, C. O'Mahony, C. M. Faulkner, M. Bosea, P. Gleeson, J. D. Holmes, and M. A. Morris, J. Phys. D Appl. Phys. **44**, 174012 (2011).

7. J. Varghese, T. Ghoshal, N. Deepak, C. O'Regan, R. W. Whatmore, M. A. Morris, and J. D. Holmes, Chem. Mater. **25**, 1458 (2013).

8. S. Malynych, I. Luzinov, and G. Chumanov, J. Phys. Chem. B. **106**, 1280 (2002).

9. C. Corten, K. Kretschmer, and D. Kuckling, Beilstein. J. Org. Chem. **6**, 756 (2010).

10. U. Borchert, U. Lipprandt, M. Bilang, A. Kimpfler, A. Rank, R. Peschka-Suss, R. Schubert, P. Lindner, and S. Forster, Langmuir. **22**, 5843 (2006).

11. D. Cho, A. Noro, A. Takano, and Y. Matsushita, Macromolecules. **38**, 3033 (2005).

12. F. S. Bates, and G. H. Fredrickson, Phys. Today. **52**, 32 (1999).

13. S. G. Jang, A. Khan, C. J. Hawker, and E. J. Kramer, Macromolecules. **45**, 1553 (2012).

14. P. Mokarian-Tabari, R. Senthamaraikannan, C. Glynn, T. W. Collins, C. Cummins, D. Nugent, C. O'Dwyer, and M. A. Morris. Nano Lett. **17**, 2973 (2017).

15. C. Cummins, and M. A. Morris, Microelectron. ENG. **195**, 74 (2018).

16. N.-G. Kang, B.-G. Kang, H.-D. Koh, M. Changez, and J.-S. Lee, React. Funct. Polym. **69**, 470–479 (2009).

17. S. Pal, Pyridine: A Useful Ligand in Transition Metal Complexes. in *Pyridine*, edited by Pandey, P. P.) (InTechOpen, 2018), pp. 57-74.

18. U. Rafique, M. Mazhar, S. Ali, and F. A. Khwaja, Synthetic. Met. **78**, 73 (1996).

19. Z. Zhang, T. Dwyer, S. M. Sirard, and J. G. Ekerdt, J. Vac. Sci. Technol. A **37**, 020905 (2019).

20. D. Berman, S. Guha, B. Lee, J. W. Elam, S. B. Darling, and E. V. Shevchenko, Acs. Nano. **11**, 2521 (2017).

21. J. W. Elam, M. Biswas, S. B. Darling, A. Yanguas-Gil, J. D. Emery, A. B. F. Martinson, P. F. Nealey,b, T. Segal-Peretz, Q. Peng, J. Winterstein, J. A. Liddle, and Y.-C. Tseng, ECS. Transactions. **69**, 147 (2015).

22. Y.-C. Tseng, Q. Peng, L. E. Ocola, D. A. Czaplewski, J. W. Elam, and S. B. Darling, J. Mater. Chem. **21**, 11722 (2011).

23. J.-P. Rueff, J. M. Ablett, D. Ceolin, D. Prieur, Th. Moreno, V. Baledent, B. Lassalle-Kaiser, J. E. Rault, M. Simon, and A. Shukla, J. Synchrotron. Radiat. **22**, 175 (2015).

24. A. Herrera-Gomez, F.S. Aguirre-Tostado, P. G. Mani-Gonzalez, M. Vazquez-Lepe, A. Sanchez-Martinez, O. Ceballos-Sanchez, R.M. Wallace, G. Conti, Y. Uritsky J. Electron. Spectrosc. **184**, 487 (2011).

25. T. Sierański, J. Mol. Model. **23**, (2017).

26. M. Snelgrove, P. G. Mani-Gonzalez, J. Bogan, R. Lundy, J.-P. Rueff, G. Hughes, P. K. Yadav, E. McGlynn, M. Morris, and R. O'Connor, J. Phys. D. Appl. Phys. - *in review 2019.*

27. P. Papadopoulos, D. Peristeraki, G. Floudas, G. Koutalas, and N. Hadjichristidis, Macromolecules. **37**, 8116 (2004).

28. R. Lundy, and et al., ACS. Omega. - *in review 2019.*

29. J. J. Lebrun, and H. Porte, Polysiloxanes. in *Comprehensive Polymer Science and Supplements*, edited by. G. Allen, and J. C. Bevington, (Pergamon, 1989), pp. 593–609

30. C. J. Brinker, J. Non-Cryst. Solids. **100**, 31 (1988).

31. A. Herrera-Gomez, M. Bravo-Sanchez, O. Ceballos-Sanchez, and M. O. Vazquez-Lepe, Surf. Interface. Anal. **46**, 897 (2014).

32. J. Muñoz-Flores, and A. Herrera-Gomez, J. Electron. Spectrosc. **184**, 533 (2012).

33. A. Herrera-Gomez, Self consistent ARXPS analysis for multilayer conformal films with abrupt interfaces. (2008).

34. O. Ceballos-Sanchez, A. Sanchez-Martinez, M. O. Vazquez-Lepe, T. Duong, R. Arroyave, F. Espinosa-Magana, and A. Herrera-Gomez, J. Appl. Phys. **112**, 053527 (2012).

35. A. Herrera-gomez, Y. Sun,*3 F.-S. Aguirre-Tostado, C. Hwang, P. G. Mani-Gonzalez, E. Flint, F. Espinosa-Magaña, and R. M. Wallace, Anal. Sci. **26**, 267 (2010).

36. T. Susi, T. Pichler, and P. Ayala, Beilstein. J. Nanotech. **6**, 177 (2015).

37. Y. Liu , Z. Jin , J. Wang , R. Cui , H. Sun , F. Peng , L. Wei , Z. Wang, X. Liang , L. Peng , and Y. Li, Adv. Funct. Mater. **21**, 986 (2011).

38. A. Mohtasebi, T. Chowdhury, L. H. H. Hsu, M. C. Biesinger, and P. Kruse, J. Phys. Chem. C. **120**, 29248 (2016).

39. M. T. Greiner, M. Festin, and P. Kruse, J. PHYS. CHEM. C. **112**, 18991 (2008).

40. G. Beamson, and D. Briggs, J. Electron. Spectrosc. **62** (1993)

41. G. Gabka, P. Bujak. K. Giedyk, K. Kotwica, A. Ostrowski, K. Malinowska, W. Lisowski, J. W. Sobczak, and A. Pron, Phys. Chem. Chem. Phys. **16**, 23082 (2014).

42. M. Barber, J.A. Connor, M. F. Guest, I. H. Hillier, and M. Schwarz, J. Chem. Soc. Farad. T. 2. **69**, 551 (1973).

43. G. Calderón-Ayala, M. Cortez-Valadez, P. G. Mani-Gonzalez, R. Britto Hurtado, J. I. Contreras-Rascón, R. C. Carrillo-Torres, Ma. E. Zayas, S. J. Castillo, A. R. Hernández-Martínez, and M. Flores-Acosta, Carbon. Lett. **21**, 93 (2017).

44. H.-W. Tien, Y.-L. Huang, S.-Y. Yang, J.-Y. Wang, and C.-C. M. Ma, C.-C. M. Carbon. **49**, 1550 (2011).

45. A. Herrera-Gomez, F. S. Aguirre-Tostado, Y. Sun, R. Contreras-Guerrero, R. M. Wallace, Y. Hisao, and E. Flint, Surf. Interface. Anal. **39**, 904 (2007).

46. S.-W. Kuo, C.-H. Wu, and F.-C. Chang, Macromolecules. **37**, 192 (2004).

47. S. U. D. Khan, B. Ahmed, S.K. Raghuvanshi, and M. A. Wahab, Indian. J. Pure. Ap. Phy. **52**, 192 (2014).

48. L. C. Cesteros, J. R. Isasi, and I. Katime, Macromolecules. **26**, 7256 (1993).

49. A. Grill, Ann. Rev. Mater. Res. **39**, 49 (2009).